An fMRI Study of Saccadic and Smooth-Pursuit Eye Movement Control in Patients with Age-Related Macular Degeneration

Deborah M. Little,[1,2,3,4,5,6] *Keith R. Thulborn,*[7] *and Janet P. Szlyk*[3,4,8]

Purpose. To compare the cortical networks that underlie oculomotor function in patients with age-related macular degeneration (AMD) with those in normally sighted control subjects, using functional magnetic resonance imaging (fMRI).

Methods. Six patients with bilateral geographic retinal atrophy due to AMD (age range, 55–83 years) were recruited for the study. The visual acuities of the patients ranged from 20/76 (0.58 logMAR) to 20/360 (1.26 logMAR). An additional six younger (age range, 22–31 years) and six older (age range, 54–78 years) normally sighted individuals were recruited as control subjects. fMRI data were acquired on a 3.0-Tesla, scanner while subjects performed visually guided saccade (VGS) and smooth-pursuit (SmP) tasks.

Results. Contrasts between VGS and fixation on a stationary target identified a network of activation that included the frontal eye fields (FEFs), supplementary eye fields (SMA/SEFs), prefrontal cortex (PFC), intraparietal sulci (IPS), and the areas of the visual cortex (MT/V5, V2/V3, and V1) in control subjects and patients. A similar network was identified for comparisons between SmP and periods of fixation. Marked variability was observed in the performance of both tasks across all patients. For both tasks, the patients generally showed increased PFC and IPS activation, with decreased activation in visual cortex compared with the control subjects. The patients showed significantly increased activation of the FEFs and SMA/SEFs in the SmP task, compared with the control subjects.

Conclusions. These data suggest that performance of both eye movement tasks required greater involvement of the cortical regions generally implicated in attention and effort in patients with AMD. (*Invest Ophthalmol Vis Sci.* 2008;49:1728–1735) DOI:10.1167/iovs.07-0372

The most common visual impairment in persons older than 50 years is a progressive loss of central visual function as a result of AMD.[1,2] It has been estimated that one in three individuals more than 75 years of age and 1 in 30 individuals more than 52 years of age are affected by AMD.[3] Previous research in our laboratory with patients having juvenile or age-related macular degeneration has demonstrated that good central visual acuity is critically important in performing everyday activities, such as reading, writing personal correspondence, and recognizing faces and expressions, and that patients with macular degeneration are impaired in these areas.[4–8]

Commonly, patients who are affected by AMD show some adaptation to their compromised visual system. This adaptation is observed clinically by the use of preferred retinal locations (PRLs) and viewing eccentrically outside of diseased foveae. The use of PRLs is effortful and fatiguing to the patients. Furthermore, many patients use different PRLs depending on the nature of the task.[9,10] Although adaptive in nature, the use of PRLs does not result in normal oculomotor function. For example, the reading rates of patients with AMD using PRLs are substantially lower than those of normally sighted subjects.[11–14] A potential reason for reduced function in patients using PRLs is abnormal scanning of text, which would involve unsteady fixation, and inaccurate saccadic and pursuit eye movements.[15–19] Confirmatory evidence for this hypothesis comes from studies of subjects reading scrolled or sequentially presented text. When the requirement for the organization and planning of eye movements during reading is reduced, patients' reading rates and accuracies are increased, although they are still slower and less accurate than those of control subjects.[20–24]

Although patients show behavioral compensation by using PRLs, oculomotor function during daily activities such as reading is still impaired. This observation suggests that oculomotor function using PRLs is quantitatively and qualitatively different from normal oculomotor function. These findings and the fact that maintenance of a PRL is an effortful process, leads to the hypothesis that the use of PRLs requires an increased reliance on higher-order cortical regions for the execution of oculomotor functions, such as with saccadic and pursuit eye movements.

The primary goal of the present study was to examine the cortical networks that underlie saccadic and pursuit eye movements in patients affected by AMD who use PRLs. To do this, patients and normally sighted control subjects performed saccadic and pursuit eye movement tasks interspersed with periods of central fixation while functional magnetic imaging data were acquired. This study provides insight into the downstream cortical consequences of retinal disease.

Methods

Participants

The research was approved by the local institutional review board and adhered to the tenets of the Declaration of Helsinki. Before participation, all subjects provided signed informed consent.

From the Departments of [1]Neurology and Rehabilitation, [2]Anatomy and Cell Biology, [3]Ophthalmology and Visual Sciences, [4]Psychology, and the Centers for [5]Stroke Research, [6]Cognitive Medicine, and [7]MR Research, University of Illinois at Chicago College of Medicine, Chicago, Illinois; and the [8]Research and Development Service of the Jesse Brown Veterans Administration Medical Center, Chicago, Illinois.

Supported by grants from the Department of Veterans Affairs Rehabilitation Research and Development Service, Washington, DC; Washington Square Health Foundation, Chicago, IL; and Research to Prevent Blindness, Inc., New York, NY.

Submitted for publication March 28, 2007; revised September 18 and December 10, 2007; accepted February 20, 2008.

Disclosure: **D.M. Little**, None; **K.R. Thulborn**, None; **J.P. Szlyk**, None

The publication costs of this article were defrayed in part by page charge payment. This article must therefore be marked "*advertisement*" in accordance with 18 U.S.C. §1734 solely to indicate this fact.

Corresponding author: Deborah M. Little, Department of Neurology and Rehabilitation; 1645 W. Jackson, Suite 400; Chicago, IL 60612; little@uic.edu.

Patients

We included six patients (three women, three men) with AMD, ranging in age from 55 to 83 years. (An additional two patients and two younger control subjects and one older were enrolled but were later excluded due to excessive head motion. The criterion for this decision is presented in the section entitled data screening and image preprocessing.) Visual acuities in the patients' better eyes ranged from 20/76 (0.58 logMAR) to 20/360 (1.26 logMAR). All the patients had bilateral geographic atrophy. and all were using an eccentric PRL, as determined from fundus fixation photographs. This procedure has been used in a previous publication.[24] More information regarding their vision status is provided in the Results section.

Control Subjects

We recruited six younger and six older normally sighted control subjects. The younger control group consisted of three women and three men, ranging in age from 22 to 31 years (median, 25). The older control group consisted of four women and two men, ranging in age from 54 to 78 years (median, 73). All the normally sighted control subjects had corrected vision of at least 20/20 in both eyes.

Experimental Methods

Sequence of Experiments. The study consisted of a single training and eye-movement–monitoring session followed by fMRI data acquisition. In the training session, the patients and control subjects were given instructions on the visually guided saccade (VGS) and smooth-pursuit (SmP) tasks that they would be encountering within the scanner during the imaging session. Before imaging, the patients were given practice on the tasks. Although the eye movements were not measured, they were monitored during fMRI data acquisition to ensure that the patients and control subjects were performing the tasks (MRIχ Technologies, Bannockburn, IL).

Imaging Tasks. *Visually Guided Saccade Task.* The VGS task required the subject to follow a dot (subtending 2° of visual angle) that was presented in one of seven possible locations (at 3°, 6°, or 9° on either side of a center 0° location). This target size was chosen so that patients with better than 20/600 vision would be able to follow the dot. Every 3 seconds, the position of the dot moved to the position immediately 3° to either the left or right of the previous position. The probability of the dot's appearing at the position 3° to the left or right was set to 0.5, with the exception being if the target was located at ±9°, in which case the next target location would predictably be located at ±6°. To ensure their sustained attention, the subjects were required to indicate (by pressing a response button) when the dot changed to a cross (also subtending 2°). The VGS task was presented in 30-second blocks interspersed with 30 seconds of fixation on a stationary target located at the 0° position for six cycles.

Smooth-Pursuit Task. The SmP task required the subject to follow a dot (subtending 2° of visual angle, equivalent to a 20/600 stimulus) that moved in a sinusoidal fashion beginning at 0°, moving to the extreme positions (at 9°) on the left, and then 9° on the right. The total time taken for one oscillation of movement was 5 seconds.

This paradigm was also presented as a block design with 30 seconds of fixation on a stationary target located at 0° followed by 30 seconds of the smooth-pursuit condition (both the fixation stimulus and the dot subtended 2°), for a total of six cycles of both conditions.

Imaging Parameters. A 3.0-Tesla whole-body scanner (Excite ver. 2.0; GE Healthcare, Waukesha, WI) using serial gradient-echo, echo-planar imaging (plane, axial; TR, 2999 ms; TE, 30.7 ms; flip angle, 90°; NEX, 1; bandwidth, 62 kHz; voxel size, 3.125 × 3.125 × 3 mm; acquisition matrix, 64 × 64; FOV, 20 × 20 cm^2; slice thickness/gap, 3/1 mm/mm; slices, 34) was used for all image acquisition. The paradigms were presented in the scanner on a visor[25] and coordinated with behavioral and physiological measurements (MRIχ Technologies).

After the completion of each functional imaging session, a single three-dimensional (3-D), high-resolution anatomic scan was acquired (3-D inversion recovery fast spoiled gradient recalled [3D IRfSPGR]; plane, axial; TR, 9 ms; TE, 2.0 ms; flip angle, 25°; NEX, 1; bandwidth, 15.6 kHz; acquisition matrix, 256 × 256; FOV, 22 × 16.5 cm^2; slice thickness/gap, 1.5/0 mm/mm; slices, 124).

Imaging Analysis. A series of analyses was performed on the image data for the younger control subjects ($n = 6$), the older control subjects ($n = 6$), the group of patients with AMD, and each patient with AMD for each task (i.e., VGS and SmP). We describe the preprocessing performed on the individual data and our methods for identifying relevant regions of interest (ROI). After this, we describe a series of analyses that were conducted to identify the regions involved in completing the tasks for younger control subjects, older control subjects, and patients with AMD and to quantify the response within each of these major regions (frontal eye fields, FEFs; supplementary eye fields, SMA/SEFs; intraparietal sulci, IPS; visual association regions including primary, V1; secondary and tertiary, V2/V3; and visual motion regions, MT/V5; and areas in the prefrontal cortex, PFC). A random-effects analysis (with individual subjects treated as random effects) was then performed on the younger control subjects and separately on older control subjects and patients with AMD, to detect significant ROIs. Direct comparisons between control subjects and groups of patients were also performed (two-sample, voxel-wise comparisons). These group analyses were followed with extraction of our primary dependent measure (volume of activation) from the ROIs applied to the data from individuals.

Data Screening, Image Preprocessing, and Statistical Analysis

Before any statistical processing, the data were screened for excessive head motion, as calculated within AFNI.[26] Data exceeding 3 mm of in-plane head motion were excluded from further analysis. The application of this criterion excluded data from two additional patients and two younger control subjects and one older. Data from these five subjects are not reported in any other portion of this article. The final sample included six patients with AMD and six younger and six older control subjects. In addition, the first complete cycle of the tasks was excluded from further analyses, to ensure acclimation to the scanning environment.

The fMRI data were preprocessed on a voxel-wise basis in FIASCO[27] before the calculation of any statistics. After the drift was corrected, outliers were identified and excluded from further analysis. An outlier was defined as any image in the time series data that fell 2.5 SD from the mean of the series. To be included in further analysis, we required that at least 50 volumes of fixation and 50 volumes of the eye movement task remain after our outlier censorship. This criterion excluded one additional older control. A 3-D head-motion correction[26] was then applied to the remaining data.

To determine the *extent of activation*, we calculated voxel-wise *t*-statistics for BOLD contrast between the eye movement and stationary fixation conditions for each paradigm in FIASCO.[27] To accommodate the shape of the hemodynamic response, we discarded data from the first 6 seconds of each 30-second block.[28] To control for multiple comparisons, we applied a false discovery rate (FDR) of 0.05 to the data from each subject. The FDR controls for the proportion of false positives among only those voxels that exceed the statistical threshold and therefore reduces the likelihood of type I errors.[29] The data were then imported into AFNI[26] and transformed into Talairach-Tournoux coordinates. This step involves interpolation of the data. A cluster threshold requiring nine contiguous (in any direction) active voxels (equivalent to three voxels in original image space) was then applied.[30] The interpolated functional data were then smoothed by using an isotropic Gaussian kernel (full width at half maximum [FWHM] = 3 mm^3). A random-effects analysis was performed separately on the groups of younger control subjects, older control subjects, and patients with AMD. The group data for both younger and older control subjects was thresholded at $P = 0.05$.

In addition to the voxel-based comparisons, a set of analyses was conducted to determine whether the volume of activation for each

patient differed from that of the entire group of control subjects. Because of the relatively small group of control subjects ($n = 12$), we chose to use a modified version of the *t*-test that allows the comparison of a single sample to a population, while taking into account the sample size of that population[31,32]:

$$t = \frac{X_1 - \bar{X}_2}{s_2 \sqrt{\frac{N_2 + 1}{N_2}}},$$

where X_1 is the value of the individual patient with AMD and X_2, S_2, and N_2 are the means, SD, and sample size of the control subjects and where the degrees of freedom for t are defined as:

$$df = N_2 - 1$$

ROI Identification and Analysis

Random-effects analyses were conducted on the normalized maps for the group of six younger control subjects and (separately) for the group of six older control subjects. To determine the ROIs that were implicated in each paradigm, we conducted a mixed-effects analysis on the normalized activation maps for these groups of subjects, so that those clusters that were significantly implicated during the experimental protocol were identified. The clusters of activated voxels were localized to brain regions that are commonly recognized as part of the visuospatial network, including the left and right FEFs, SMA/SEFs, left and right parietal lobules along the IPS, and visual cortical regions (V1, V2, and V3 and V5/MT). Because the paradigms do not separate activation between V2 and V3, the regions of V2 and V3 were combined. Based on these analyses and the resultant activation maps and the neuroimaging literature reporting tasks similar to those used in these experiments, we defined the anatomic boundaries of these ROIs to characterize the extent of task-related activation. These regions were first identified on the averaged anatomic image from the left and right FEFs and were defined to include the precentral sulci and immediately adjacent gyri.[33] The SMAs, including the SEFs were identified as the tissue anterior to the precentral sulcus along the medial frontal lobes and posterior to the caudate nucleus.[34] The superior parietal lobule was drawn superior to the IPS and posterior to the postcentral sulcus,[34,35] left and right superior parietal lobule (superior and anterior to the intraparietal sulcus and posterior to the postcentral sulcus),[35] left and right inferior parietal lobule (inferior and posterior to the intraparietal sulcus including the supramarginal gyrus),[36] primary and secondary visual cortices (along the calcarine fissure to the cuneus and lingual gyrus),[37] tertiary visual cortex (from the borders of V1/V2 to the middle occipital gyrus),[37] and fusiform gyrus (from the mammillary body to the anterior tip of the parieto-occipital sulcus).[38] We broadly defined the PFC using Brodmann's definitions to include the area between the superior rostral sulcus and inferior rostral sulcus and dorsally by the anterior cingulate. These ROIs were then applied to the individual data so that the number of interpolated voxels (volume of activation) could be calculated for each ROI for each subject for each paradigm.

Results

Visually Guided Saccades

Representative slices depicting regions implicated during the VGS task in the group of the younger control subjects (Fig. 1B), the group of older control subjects (Fig. 1C), and the group of patients with AMD (Fig. 1D) are presented in Figure 1. Visual inspection of these activation maps suggests that the younger and older control subjects both showed activation bilaterally in the FEFs, SMA/SEFs, superior and inferior parietal lobules, and the visual cortices. In contrast, the activation map for the group of patients with AMD showed marked reduction of

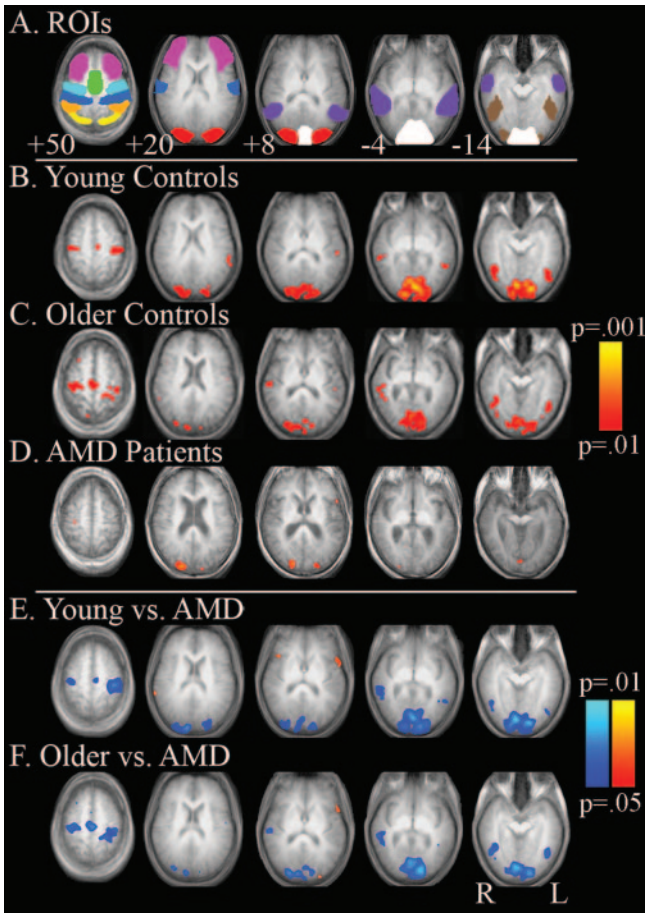

Figure 1. Significant regions of activation that showed increased activity during the VGS task compared with fixation. The ROIs are presented in (**A**) and include the inferior parietal lobule (*yellow*), superior parietal lobule (*orange*), SMA/SEFs (*green*), dorsolateral PFC (*pink*), FEFs (*light blue*), primary motor area (*dark blue*), V3 (*red*), medial temporal lobule (V5/MTl; *purple*), fusiform gyrus (*brown*), and primary visual cortex (V1/V2; *white*). Activation maps are presented for the groups of younger control subjects (**B**), older control subjects (**C**), and patients with AMD (**D**) and for comparisons between the younger control subjects and patients with AMD (**E**) and between the older control subjects and patients (**F**). (**B–F**) *Blue*: regions with greater activation in the control subjects; *red*: regions with greater activation in the patients.

activation with significant clusters being present only in the parietal lobules. Voxel-wise between-group comparisons between the younger control subjects and patients with AMD (Fig. 1E) and between the older control subjects and patients with AMD (Fig. 1F) confirm this observation, with both groups of control subjects showing greater activation in the FEFs, SMA, superior and inferior parietal lobules, and visual cortices. Of note is a region of increased activity in the left ventrolateral PFC in the patients with AMD, relative to both groups of control subjects.

More discrete ROI analyses were conducted on all these significant regions of activation (FEFs and SEFs, parietal lobules, and visual cortices). Because of a priori hypotheses regarding cortical control in patients with degraded sensory input, we also included an ROI analysis on the PFC. These data are presented in Figure 2. As there were no significant differences in the volume of activation between the left and right hemispheres, the volume of activation within each ROI is presented collapsed across the two hemispheres in Figure 2.

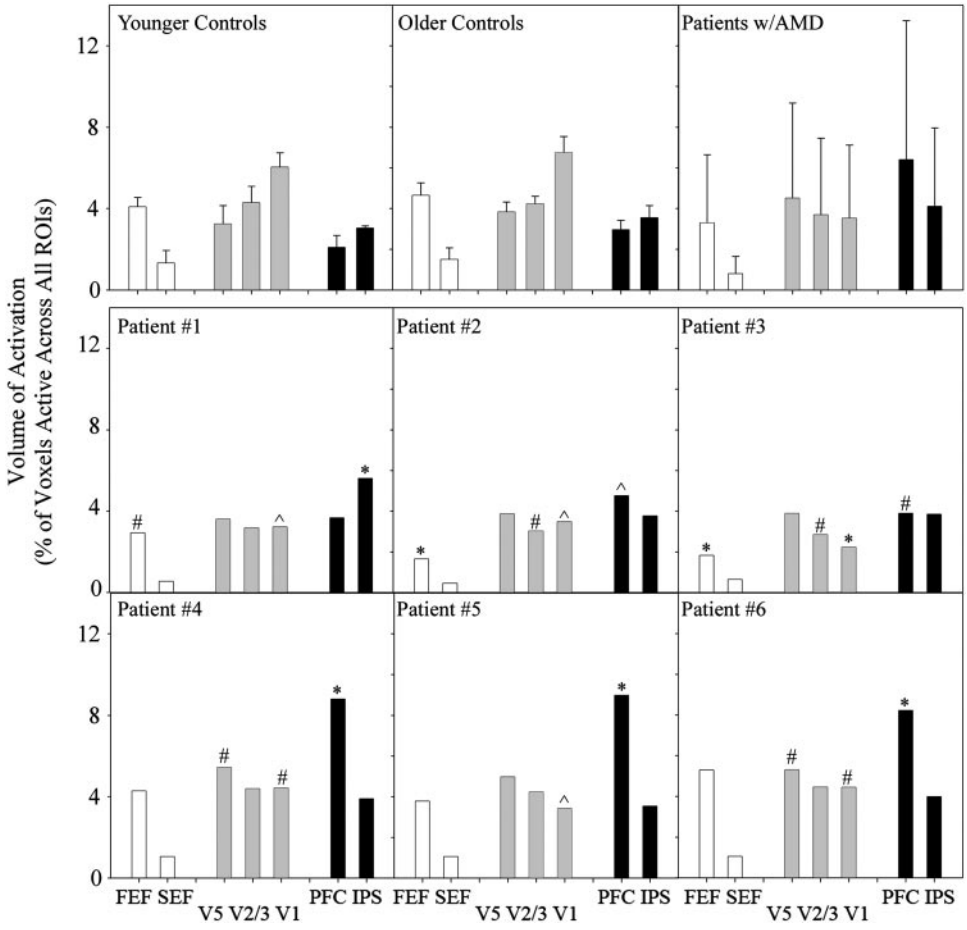

FIGURE 2. Volumes of activation presented as the percentage of voxels exceeding a threshold of $P = 0.05$ during performance of the VGS task for the younger control subjects, older control subjects, patients with AMD, and patients 1 to 6. Error bars, 1 SE. Significant comparisons between individual patients and the control subjects are indicated above each bar: #$P < 0.05$; ^$P < 0.01$; *$P < 0.001$.

ROI data did not identify any significant differences between the groups of younger and older control subjects (FEF, $P = 0.86$; SMA/SEF, $P = 0.72$; V5, $P = 0.12$; V2/V3, $P = 0.53$; V1, $P = 0.24$; PFC, $P = 0.10$; IPS, $P = 0.09$). ROI analyses on the group of patients with AMD demonstrate marked variability in each region (observed as dramatically increased error bars relative to the groups of control subjects). Because of the increased variability, we conducted a case-series analysis on the ROI data (Fig. 2) and on the image data (Fig. 3) for each patient. Because there were no significant differences between older and younger control subjects, and for ease of presentation, we collapsed these groups for the statistical comparisons and also in Figure 3A. The voxel with the maximum *z*-score within each ROI for this group data and the corresponding size of the ROI are presented in Table 1.

Representative slices depicting regions implicated during the VGS task in the group of control subjects (including both younger and older control subjects) and in each patient with AMD are presented in Figure 3. Overall, the patients with AMD showed a different distribution of cortical activation relative to control subjects. In addition, all but one of the individual patients showed increased prefrontal activation (the final patient showed a trend for increased PFC activation) relative to control subjects. A discussion of each patient's activation pattern and how each patient compares with control subjects follows. Significant comparisons relative to the group of control subjects is indicated on Figure 3.

Patient 1. Patient 1 was a 76-year-old woman (visual acuity in the better eye [OD] = 0.78 logMAR; 20/121; OS = 0.92 logMAR; 20/166; duration of AMD, 3 years). Consistent with control subjects, Figure 3B shows activation during performance of the VGS task, which includes clusters of activation identified to include SMA/SEFs, IPS, V1, V2/V3, and V5/MT. The ROI analyses presented in Figure 2 show that the activation in FEF was reduced compared with that in control subjects. In contrast to that in the control subjects, large volumes of activation were observed in regions within the IPS. Although there was a trend for an increase in PFC, the observation did not reach significance ($P = 0.06$). Reductions in activation were observed in primary visual cortical regions.

TABLE 1. ROIs, Their Corresponding Broadmann Areas, the Size of Each ROI, and the Coordinates of the Center of each ROI

	BA	ROI Size*	*x*	*y*	*z*
Prefrontal Cortex (PFC)	45				
Left		58,358	−33	−33	36
Right		55,796	34	−35	35
Frontal Eye Fields (FEF)	8				
Left		23,542	42	−6	44
Right		24,496	−43	−5	43
Visual Cortex (V1/V2)	17/18				
Left		21,848	10	−88	−8
Right		21,856	−11	−88	−8
Supplementary Eye Fields (SEF)	6				
Left		6,613	5	8	53
Right		7,306	−5	8	52
Visual Cortex (V3)	19				
Left		14,663	24	−88	16
Right		14,662	−23	−89	17
Inferior Parietal (IPS)	42				
Left		26,409	48	−41	39
Right		26,690	−49	−41	39

BA, Brodmann area

* Data are expressed in cubic millimeters.

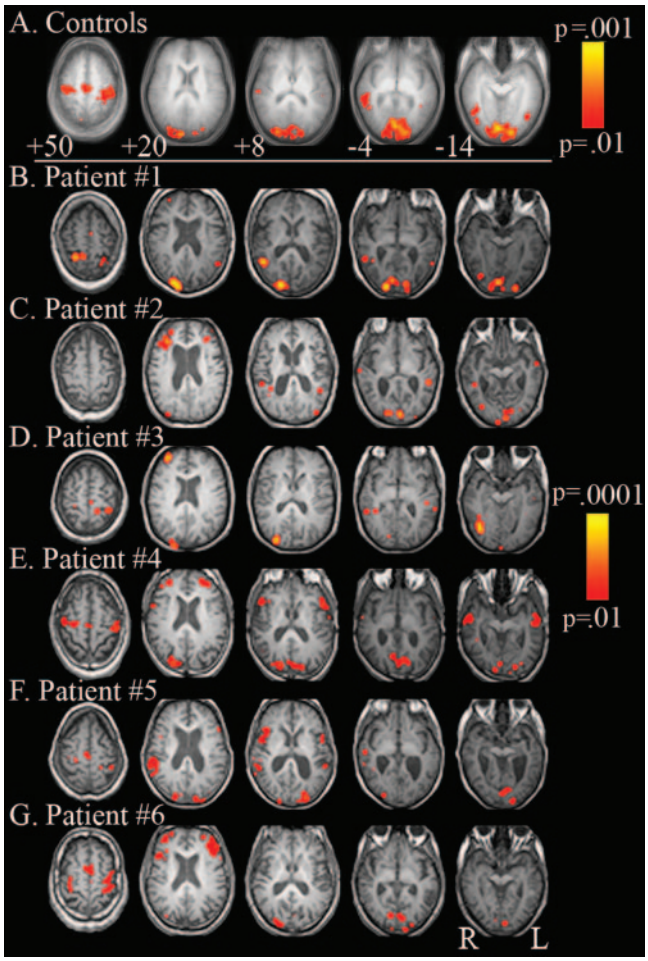

FIGURE 3. Activation maps including representative slices for the group of control subjects (younger and older) are presented in (**A**) for the VGS task. (**B**–**G**) show activation maps for six individual patients.

Patient 2. Patient 2 was an 83-year-old man (visual acuity in the better eye [OD] = 0.94 logMAR; 20/174; OS = 1.30 logMAR; 20/400; duration of AMD, 11 years; Fig. 3C). Regions of activation were observed in the IPS, but with more activation in the superior parietal than in the IPS, V1, V2/V3, and MT/V5. Consistent with the findings in patient 1 (Figs. 2, 3), there was increased activity, relative to control subjects, in the PFC; a trend for increased IPS activation ($P = 0.062$); and reduced activation in FEFs, V2/V3, and V1.

Patient 3. Patient 3 was a 55-year-old woman (visual acuity in the better eye [OD] = 1.26 logMAR; 20/360; OS = 1.36 logMAR; 20/450; duration of AMD, 5 years). Activation, presented in Figure 3D and plotted in Figure 2, was observed in PFC, IPS, V1, V2/V3, and MT/V5. As with patient 2, there was increased activity, relative to control subjects, in the PFC; a trend for increased IPS activation ($P = 0.07$); and reduced activation in FEFs, V2/V3, and V1.

Patient 4. Patient 4 was a 64-year-old man (visual acuity in the better eye [OD] = 0.58 logMAR; 20/76; OS = 0.66 logMAR; 20/91; duration of AMD, 4 years; Fig. 3E). Activation was observed bilaterally in the FEFs, the SEFs, the IPS, V1, V2/V3, and the PFC. Relative to the control subjects, patient 4 showed increased activation in V5/MT and the PFC and reduced activation in V1.

Patient 5. Patient 5 was an 82-year-old woman (visual acuity in the better eye [OD] = 1.20 logMAR; 20/320; OS = 1.44; 20/560; duration of disease, 3 years; Fig. 3F). Activation was observed bilaterally in the FEFs; SEFs; along the IPS, V1, and V2/V3 areas; and in the PFC. Activation in V1 was reduced relative to control subjects and increased in the PFC. There was a trend for a reduction in FEFs and for an increase in V5 activation, but neither reached significance (respectively, $P = 0.06$ and $P = 0.07$).

Patient 6. Patient 6 was a 70-year-old man (visual acuity in the better eye [OD] = 0.58 logMAR; 20/76; OS = 0.74; 20/110; duration of AMD = 2 years; Fig. 3G). Activation was observed bilaterally in the FEFs; SEFs; along the IPS, V1, and V2/V3 areas; and in the PFC (Fig. 2). Similar to the pattern of activation in patient 4, there was increased activation in V5/MT and the PFC and reduced activation in V1 relative to control subjects.

Overall, there was an increase in prefrontal activation for all the patients compared to the control subjects, although this observation reached significance in five of six patients. In addition, there is a change in the relationship between activation in V1, V2, and V3 compared with activity in V5/MT. Specifically, the patients showed increased activation in MT/V5 relative to V1 whereas the control subjects showed greater activation in V1 relative to MT/V5.

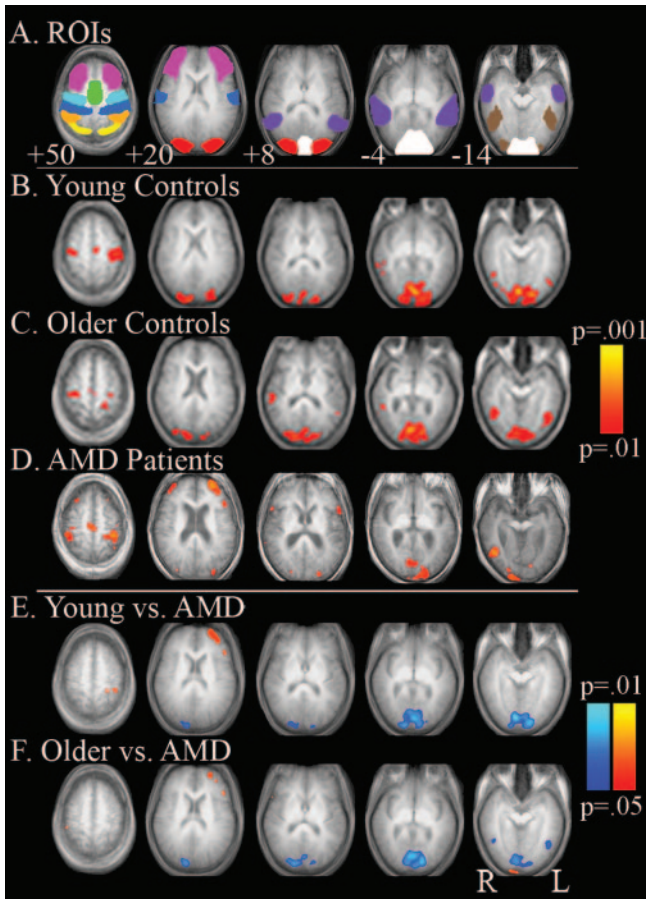

FIGURE 4. Significant regions of activation that showed increased activity during the SmP task compared with central fixation. The ROIs are presented in (**A**) and include the inferior parietal lobule (*yellow*), superior parietal lobule (*orange*), SMA/SEFs (*green*), dorsolateral PFC (*pink*), FEFs (*light blue*), primary motor area (*dark blue*), V3 (*red*), medial temporal lobule (V5/MT); *purple*), fusiform gyrus (*brown*), and primary visual cortex (V1/V2; *white*). Activation maps are presented for the groups of younger (**B**) and older (**C**) control subjects and patients with AMD (**D**) and for comparisons between the younger control subjects and the patients (**E**) and between the older control subjects and the patients (**F**). (**B**–**F**) *Blue*: regions with greater activation in the control subjects; *red*: regions with greater activation in the patients.

Smooth Pursuit

Representative slices depicting regions implicated during the SmP task in the group of younger control subjects (Fig. 4B), the group of older control subjects (Fig. 4C), and in the group of patients with AMD (Fig. 4D) are presented in Figure 4. Random-effects analyses on the groups of younger and older control subjects demonstrated significant activation bilaterally in the FEFs, SMA/SEFs, superior and inferior parietal lobules, and the visual cortices. Similar to the control subjects, patients with AMD showed activation in the FEFs, SMAs, parietal lobules, and visual cortex. Additional clusters of activation were observed bilaterally in the PFC. Voxel-wise between groups comparisons between the younger control subjects and patients (Fig. 4E) and between the older control subjects and patients (Fig. 4F) demonstrate no apparent difference in frontal or SEFs. Both groups of control subjects showed greater activation in parietal lobules and in visual cortex. The patients showed increased activation bilaterally in the PFC.

As with the VGS, more discrete ROI analyses were conducted on all these significant regions of activation (FEFs and SEFs, parietal lobules, and visual cortices). These data are presented in Figure 5.

ROI data did not identify any significant differences between the groups of younger and older control subjects (FEF, $P = 0.94$; SEF, $P = 0.88$; V5, $P = 0.72$; V2/V3, $P = 0.13$; V1, $P = 0.10$; PFC, $P = 0.82$; IPS, $P = 0.92$). ROI analyses on the group of patients with AMD demonstrate marked variability in each region (observed as dramatically increased error bars relative to the groups of control subjects).

Qualitative inspection of the representative slices presented in Figure 4 illustrates greater similarities between patients and control subjects during the smooth-pursuit task compared with the differences observed for the VGS. Unlike for the VGS, all the patients with AMD showed significant activation in the FEFs and SMA/SEFs (Figs. 5, 6). In fact, all but one patient showed significantly increased activation in the FEFs compared with the control subjects. Similarly, all the patients showed a trend for greater activity in the SMA/SEFs than did the control subjects. In addition, all the patients showed increased activation in the PFC and IPS relative to control subjects.

Overall, the patients showed greater activation in the prefrontal and parietal regions than did both groups of control subjects. During performance of SmP, the AMD patients showed increased activity in the FEFs and a trend for increased activation in the SEFs, compared with the control subjects.

Comparison of VGS and SmP

Voxel-wise comparisons between the VGS and SmP were conducted on the image data for each group of subjects and are presented in Figure 7. Overall, there was great similarity between the VGS and SmP in both groups of control subjects. A discussion of the regions that were significantly different follows. The younger control subjects showed increased activation in the superior and inferior parietal regions during the VGS task and increased activation in the visual cortices (V1, V2/V3) during SmP. The older control subjects showed increased activation in the visual cortices (V1, V2/V3, and V5) during VGS and increased activation in the PFC during the SmP. Consistent with the results presented separately for the VGS and SmP tasks, patients with AMD showed increased activation in the FEFs, SMA/SEFs, PFC, and visual cortices (V1, V2/V3, and MT)

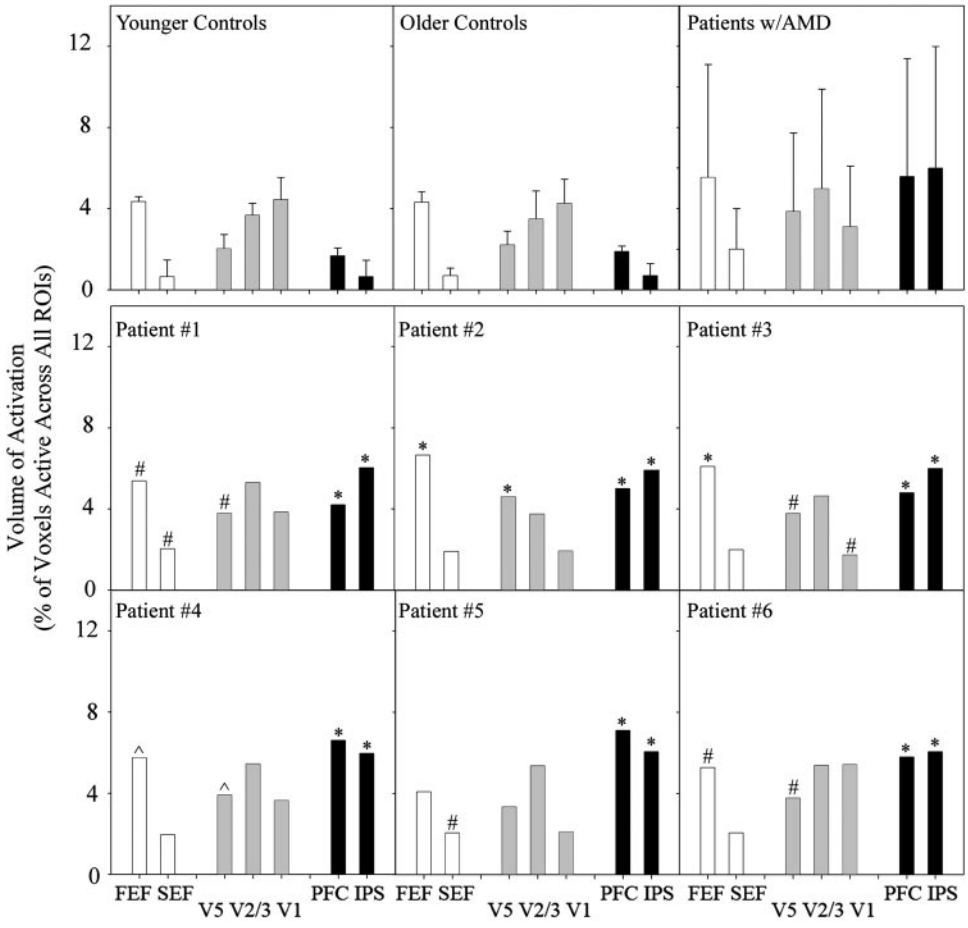

FIGURE 5. Volumes of activation presented as the percentage of voxels exceeding a threshold of $P = 0.05$ during performance of the SmP task in the younger control subjects, older control subjects, group of patients with AMD, and patients 1 to 6. Error bars, SE. Significant comparisons between the individual patient and control subject values are indicated above each bar: $\#P < 0.05$; $\wedge P < 0.01$; $*P < 0.001$.

during SmP. A single cluster of voxels was found to show an increase during VGS relative to SmP in the right inferior parietal lobule in patients with AMD.

Discussion

The VGS task demand a search for and identification of a target situation in quasi-random locations. In contrast, the SmP task demands maintenance of a smoothly, and therefore predictably, moving target on the PRL. The cortical networks that subserve these tasks do not have large differences across the regions tested between younger and older normally sighted subjects. The VGS task has greater PFC and IPS activation than does the SmP task in normally sighted older control subjects, presumably due to the greater demands associated with finding and identifying an unpredictable target. The oculomotor activation in FEF and SEF was not different for the two tasks in either group of control subjects. In contrast, the AMD patients showed considerable variability in activation patterns across individual patients, presumably reflecting different patient skills, although all could perform the tasks.

The greater activation in cognitive aspects (PFC, IPS) relative to motor aspects (FEF, SEF) of the networks for both tasks compared to that in normally sighted subjects is consistent with the greater demands imposed by degraded visual input and the use of alternative strategies for locating and identifying a target. Patients with macular degeneration can adapt to the compromised visual input by using noncentral PRLs. The incongruence of gaze location and visual processing, usually closely associated in normal-sighted individuals, results in reduced performance on basic oculomotor tasks. Difficulties with such basic functions also impact higher order cognitive tasks, such as reading, that require coordination of sequential eye movement with the processing of the visual information.

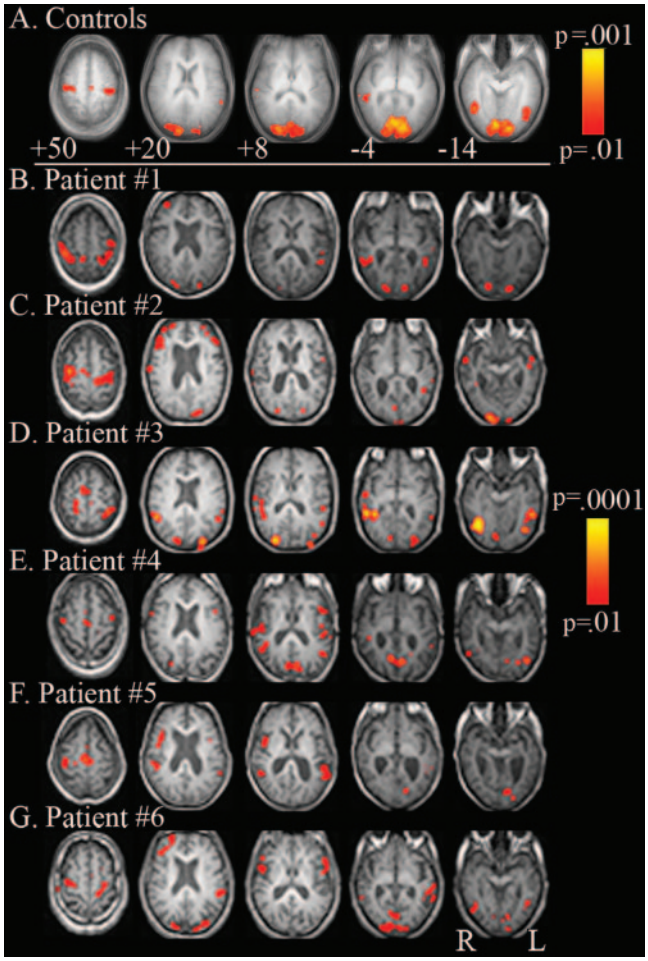

Figure 6. Activation maps including representative slices for the groups of younger and older control subjects are presented in (**A**) for the SmP task. (**B–G**) Activation maps for each patient.

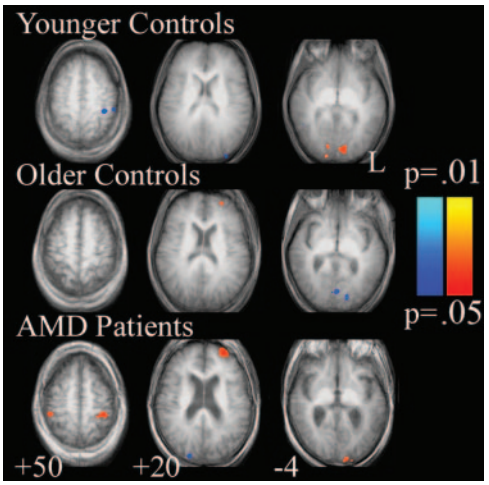

Figure 7. Voxel-wise comparisons between VGS and SmP in the younger and older control subjects and in the patients. *Blue*: regions with increased activation during the VGS relative to SmP; *red*: regions with increased activation during SmP relative to VGS.

Although the presently used tasks have not been previously reported in patients with AMD, the finding of alterations in underlying cortical networks in otherwise healthy adults is consistent with those in two recent studies.[39,40] Sunness et al.[40] investigated whether the cortical areas typically activated by photograph stimulation to the scotomatous region of the retina could adapt and become activated by stimulation to more peripherally located nonscotomatous regions. The research represented a case study of one 60-year-old patient with bilateral geographic atrophy due to AMD. The authors used an expanding annulus stimulus of black-and-white contrast that reversed at 8 Hz. The results showed a lack of activity in visual cortical regions corresponding to the retinal atrophy.

In contrast, Baker et al.[39] found evidence of activation within cortical areas corresponding to the scotomatous foveal region of the retina in two patients in their sixth decade of life with long-standing juvenile-onset macular degeneration. The activation occurred when the patients were exposed to natural images of faces, objects, and scenes presented to the more peripheral retina.

Beyond a shared finding of alterations in cortical activation relative to control subjects, the present findings cannot be directly compared to these previously published findings. The goal of the present research was not to focus on retinotopic mapping of the visual cortex, but to investigate the brain activation networks that are associated with oculomotor control and function in patients with AMD who are using a retinal location other than the fovea for viewing. The present data represent a first step toward understanding the cortical and neuronal changes that occur as a result of decreased vision in patients with AMD during the performance of basic oculomotor tasks.

Acknowledgments

The authors thank Kenny Israni, BS, Jing Ming, BS, and Silvia Shin, BS for help with data collection and analysis.

References

1. Bressler N, Bressler S, Fine S. Age-related macular degeneration. *Surv Ophthalmol*. 1988;32:375–413.
2. Klein R, Klein B, Tomany S, et al. Ten-year incidence and progression of age-related maculopathy: The Beaver Dam eye study. *Ophthalmology*. 2002;109:1767–1779.
3. Klein R, Klein B, Jensen S, Meuer S. The five-year incidence and progression of age-related maculopathy: the Beaver Dam Eye Study. *Ophthalmology*. 1997;104:7–21.
4. Szlyk J, Fishman G, Alexander K, et al. Relationship between difficulty in performing daily activities and clinical measures of visual function in patients with retinitis pigmentosa. *Arch Ophthalmol*. 1997;115:53–59.
5. Szlyk J, Fishman G, Aslan R, Grover S. Legal blindness and employment in patients with juvenile-onset macular dystrophies or achromatopsia. *Retina*. 1998;18:360–367.
6. Szlyk J, Fishman G, Grover S, et al. Difficulty in performing everyday activities in patients with juvenile macular dystrophies: comparison with patients with retinitis pigmentosa. *Br J Ophthalmol*. 1998;82:1372–1376.
7. Szlyk J, Seiple W, Fishman G, et al. Perceived and actual performance of daily tasks: relationship to visual function tests in individuals with retinitis pigmentosa. *Ophthalmology*. 2001;108:65–75.
8. Szlyk J, Stelmack J, Massof R, et al. Performance of the veterans affairs low vision visual functioning questionnaire (VA LV VFQ). *J Vis Impair Blindness*. 2004;98:261–275.
9. Deruaz A, Whatham A, Mermoud C, Safran A. Reading with multiple preferred retinal loci: implications for training a more efficient reading strategy. *Vision Res*. 2002;42:2947–2957.
10. Lei H, Schuchard R. Using two preferred retinal loci for different lighting conditions in patients with central scotomas. *Invest Ophthalmol Vis Sci*. 1997;38:1812–1818.
11. Knoblauch K, Arditi A, Szlyk J. Effects of chromatic and luminance contrast on reading. *J Opt Soc Am A Opt Imag Sci*. 1991;8:428–439.
12. Legge G, Ross J, Isenberg L, LaMay J. Psychophysics of reading: clinical predictors of low-vision reading speed. *Invest Ophthalmol Vis Sci*. 1992;33:677–687.
13. Rayner K, Bertera J. Reading without a fovea. *Science*. 1979;206:468–469.
14. Whittaker S, Lovie-Kitchin J. Visual requirements for reading. *Optom Vis Sci*. 1993;70:54–65.
15. Cummings R, Whittaker S, Watson G, Budd J. Scanning characters and reading with a central scotoma. *Am J Optom Physiol Opt*. 1985;62:833–843.
16. Fletcher D, Schuchard R. Preferred retinal loci relationship to macular scotomas in a low-vision population. *Ophthalmology*. 1997;104:632–638.
17. Sunness J, Applegate C, Haselwood D, Rubin G. Fixation patterns and reading rates in eyes with central scotomas from advanced atrophic age-related macular degeneration and Stargardt disease. *Ophthalmology*. 1996;103:1458–1466.
18. White J, Bedell H. The oculomotor reference in humans with bilateral macular disease. *Invest Ophthalmol Vis Sci*. 1990;31:1149–1161.
19. Whittaker S, Cummings R, Swieson L. Saccade control without a fovea. *Vision Res*. 1991;31:2209–2218.
20. Culham L, Fitzke F, Timberlake G, Marshall J. Use of scrolled text in a scanning laser ophthalmoscope to assess reading performance at different retinal locations. *Ophthalmic Physiol Opt*. 1992;12:281–286.
21. Petre K, Hazel C, Fine E, Rubin G. Reading with eccentric fixation is faster in inferior visual field than in left visual field. *Optom Vis Sci*. 2000;77:34–39.
22. Rubin G, Turano K. Low vision reading with sequential word presentation. *Vision Res*. 1994;34:1723–1733.
23. Seiple W, Szlyk J, McMahon T, et al. Eye movement training for reading in patients with age-related macular degeneration. *Invest Ophthalmol Vis Sci*. 2005;46:2886–2896.
24. Xing J, Gerstein G. Simulation of dynamic receptive fields in primary visual cortex. *Vision Res*. 1994;34:1901–1911.
25. Thulborn K. Visual feedback to stabilize head position for fMRI. *Mag Res Med*. 1999;41:1039–1043.
26. Cox R. AFNI: software for analysis and visualization of functional magnetic resonance neuroimages. *Comput Biomed Res*. 1996;29:162–173.
27. Eddy W, Fitzgerald M, Genovese C, et al. *Functional Image Analysis Software: Computational Olio*. Heidelberg, Germany: Physica-Verlag; 1996.
28. Cohen M. Parametric analysis of fMRI data using linear systems methods. *Neuroimage*. 1997;6:93–103.
29. Genovese C, Lazar N, Nichols T. Thresholding of statistical maps in functional neuroimaging using the false discovery rate. *Neuroimage*. 2002;15:870–878.
30. Forman S, Cohen J, Fitzgerald M, et al. Improved assessment of significant activation in functional magnetic resonance imaging (fMRI): use of a cluster-size threshold. *Mag Res Med*. 1995;33:636–647.
31. Crawford J, Howell D. Comparing an individual's test score against norms derived from small samples. *Clin Neuropsychol*. 1998;12(4):482–486.
32. Sokal R, Rohlf J. *Biometry*. San Francisco, CA: WH Freeman; 1995.
33. Grosbras M, Leonards U, Lobel E, et al. Human cortical networks for new and familiar sequences of saccades. *Cereb Cortex*. 2001;11:936–945.
34. Luna B, Thulborn K, Strojwas M, et al. Dorsal cortical regions subserving visually guided saccades in humans: an fMRI study. *Cereb Cortex*. 1998;8:40–47.
35. Dassonville P, Zhu X-H, Ugurbil K, et al. Functional activation in motor cortex reflects the direction and degree of handedness. *Proc Natl Acad Sci USA*. 1997;94:14015–14018.
36. Frederikse M, Lu A, Aylward E, et al. Sex differences in the inferior parietal lobule. *Cereb Cortex*. 1999;9:896–901.
37. DeYoe E, Carman G, Bandettini P, et al. Mapping striate and extrastriate visual areas in human cerebral cortex. *Proc Natl Acad Sci USA*. 1996;93:2382–2386.
38. Lee C, Shenton M, Salisbury D, et al. Fusiform gyrus volume reduction in first-episode schizophrenia: a magnetic resonance imaging study. *Arch Gen Psychiatry*. 2002;59:775–781.
39. Baker C, Peli E, Knouf N, Kanwisher N. Reorganization of visual processing in macular degeneration. *J Neurosci*. 2005;25:614–618.
40. Sunness J, Liu T, Yantis S. Retinotopic mapping of the visual cortex using functional magnetic resonance imaging in a patient with central scotomas from atrophic macular degeneration. *Ophthalmology*. 2004;111:1595–1598.